A Laboratory Experiment Of Wave Overtopping Over Dike On Steep Fringing Reef

Ho Duc Dat, Nguyen Quang Tao, Nguyen Trung Dung, Nguyen Van Bau, Mai Cao Tri, and Dinh Quang Cuong*

Faculty of Coastal and Offshore Engineering, Hanoi University of Civil Engineering, Hanoi, Vietnam.

* *Corresponding author. E-mail: cuongdq@huce.edu.vn*

Received: Mar. 05, 2024; Accepted: Jul. 22, 2024

This paper presents a laboratory study to investigate the wave overtopping over dike on the fringing reef with a large steep fore-reef slope. The experimented models were set up in wave flume, considering three different slopes of dike combined with various wave and still water levels and different roughness cases. The research results indicate that wave overtopping over a dike on the fringing reef depends not only on the relative crest freeboard but also on a synthetic parameter typical for the wave hydrodynamic properties of the fringing reef characteristics and the slope of the dike. An empirical equation of wave overtopping discharge for dike on the fringing reef was derived based on an equation in EurOtop2018 by adding new synthetic parameter, and the comparison of the data from the new empirical formulas with the measured data showed good agreement. The proposed equation of this paper has been applied to estimate wave overtopping discharge over dike on the fringing reef having a large steep fore-reef slope.

Keywords: dike, steep fringing reef, overtopping wave, wave flume, empirical formula.

http://dx.doi.org/10.6180/jase.202507_28(7).0010

1. Introduction

As waves propagating across fringing reefs characterized by shallow water depth, a pronounced transformation occurs, influenced by factors like triad interaction, breaking waves, bottom friction, and more. These factors contribute to a distinct wave distribution on fringing reefs, setting it apart from the wave propagation observed on gradual near-shore beaches. The study of wave hydrodynamics on fringing reefs has garnered global research interest in recent decades, as indicated by numerous studies [1–4]. The physical process of breaking incident waves on fringing reef results in a reduction in the wave energy. Serious damage and coastal inundation, however, often occur around fringing reef because the ocean waves interacting with the reefs cause wave breaking [5]. This leads to an increase in the infragravity waves and mean water levels within the fringing reefs [6]. Especially, long waves or infragravity waves (IG) with a period of 20s to 200s which are generated by the interaction of breaking wave groups with the reefs and nonlinear wave resonance interactions are formed [3, 7, 8].

In addition, a wave setup of average water level on the reef is created by wave breaking surrounding the fringing reef [9, 10]. The reflection of long waves from the fringing reef was a total reflection that makes standing waves and trapped IG wave energy and with relevant conditions can occur wave resonance across the reef flat [11]. The energy resonance of IG waves combined with an increase in mean water level on the reef flat is the main cause of large overtopping and floods in the fringing reef with low ground elevation or when fringing reef have a small reef width [1, 12, 13]. Wave overtopping is a product of wave runup surging over a shoreline of fringing reef. The wave runup is

caused by reef morphology and incident wave interaction, while the wave overtopping is determined by the ability to accommodate runup surges of the fringing reef [14].

Research about wave overtopping on structures such as dikes, breakwaters, sea walls, etc has a lot of achievements and is being applied in the calculation and design of coastal protection. Typically, various experimental investigations of wave overtopping on shoreline structures have been conducted by a large number of projects and studies [15–17]. The wave overtopping estimation of defensive structures like sea dikes is obtained by using some classical formulas [18]. These empirical prediction formulae have been modified and supplemented to be applicable to different circumstances [19]. In a recent study, an equation estimating the overtopping discharge was proposed by Altomare [20], in which the configuration of sea dikes was estimated based on the full spectrum wave characteristics at shallow foreshore.

Most of the studies on fringing reef with steep fore-reef slope mainly stop studying the hydrodynamic on the reef crest or reef flat, not mentioning the wave overtopping on finging reef whereas the wave overtopping studies have not mentioned the hydrodynamic mechanism is different on the fringing reef. Therefore, the application of such empirical formulas to defended structures on offshore islands or reef environments is still an unanswered question. Currently, there are still very few studies on wave overtopping over structure construction on the fringing reef. A typical research of a wave overtopping a structure on fringing reef is the studies wave overtopping over impermeable seawall on fringing reef by Y. Liu [21] and followed by the development of an artificial intelligence network tool for predicting wave overtopping [22]. However, wave overtopping across dikes, which is very common, has not been addressed in this study. Besides, there is a study by E. Beetham [1] with a dataset of 60,000 different numerical model scenarios that limit the occurrence of waves overtopping on finging reef, but there is no empirical formula to calculate the wave overtopping. In 2023, a part in study of Gao [23] focused on wave overtopping over seawalls on a reef flat and also provided a formula for calculating wave overtopping. The location of the dike in this study is situated in the middle of the reef flat, where wave overtopping will be influenced by waves behind the dike, unlike the case will studied in the paper, where the dike is positioned at the end of the reef flat, at the shoreline of the fringing reef. The formula in study of Gao does not account for the water depth on reef flat, a significant factor affecting wave propagation and overtopping, with water level variations on the reef flat being relatively small (less than 2.5m) compared to the

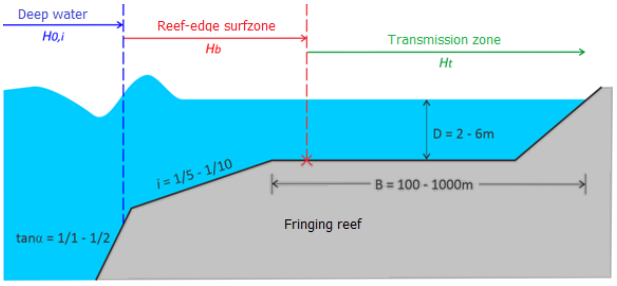

Fig. 1. Cross-section of the fringing reef (actual shape).

conditions at the fringing reefs of Vietnam, where water depth on the reef flat ranges from 2 to 6 meters. Therefore, this formula is not applicable to the case studied in the this paper.

The paper delve deeper into research and propose a formula for calculating wave overtopping over dike built at the shoreline of a fringing reef, under boundary conditions suitable for the Vietnam region. Experiment work was carried out in a 2D wave flume, in which only planar problems or wave propagation processes are considered in the direction perpendicular to the fringing reef. Three-dimensional effects due to bottom topography or oblique incident waves are not considered in this work.

2. Experiments and methods

2.1. Physical model

The experiments with the physical model were set up in a wave flume with dimensions of 45m in length, a working section that is 1.0m wide, and a height of 1.2m. This is a modern wave flume that has conducted numerous published studies [4, 24, 25] with highly accurate sensors and an Active Reflection Compensation (ARC-Deltares) system, which reduces the reflected waves from the wave absorber.

Based on the topographical survey data from several fringing reefs, the cross-sectional features quite intricate, as depicted in Fig. 1. The lower fore-reef slope is located in deep water, featuring a steep slope ranging from 1/1 to 1/2 and a water depth exceeding 40 meters in the direction of wave propagation. Moving on to the fore-reef slope, the water depth ranges from -40m to -15m, with a gentler gradient varying from 1/5 to 1/15. This region also experiences strong interaction between waves and the fringing reef. Afterward, the waves propagate into the reef flat area, which can extend from a few hundred meters to several kilometers in length, with relatively shallow water depths ranging from 2m to 6m.

The length scale of the physical model, calculated as $N_L = 40$ using Froude's scale law, is based on the charac-

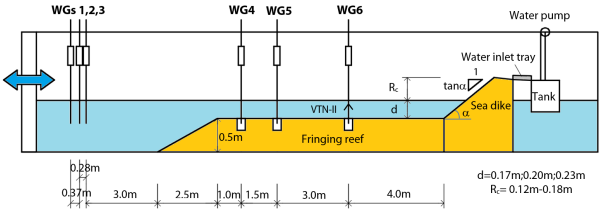

Fig. 2. Experimental layout of the physical model in the wave flume

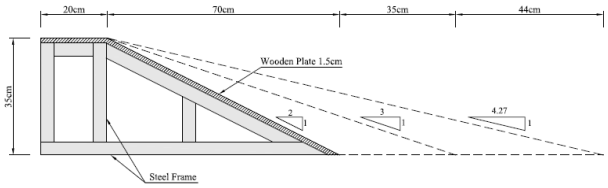

Fig. 3. Cross-sectional view of physical models with different slopes

teristics of the fringing reef and the wave flume capacity. The model's time scale is consequently $N_T = 6.32$.

The experimental setup is illustrated in Figure 2, showing a fringing reef model with a height of 0.50 m and a width of $B = 9.5$ m (380 m in the prototype condition), covered by smooth concrete mortar. This study focuses exclusively on a fore-reef slope of i $= 1/5$. According to the findings of Tuan and Cuong in 2019 [25], this value exhibits slight impact on wave hydrodynamics in fringing reefs, when varied within the range $i = 1/5$ to $1/10$.

The wave-overtopping experiments are conducted with three models (MH1, MH2, and MH3) with different slopes, $\tan\alpha = 1/2, 1/3, 1/4.27$. Besides, another model is copied from MH1 $(\tan\alpha = 1/2)$, yet has a bottom roughness (denoted as MH1-R) (see Table 1). All physical models have a height of 0.35 m , and the inclined surface consists of wooden planks (see Figure 3).

Six wave gauges are arranged in all three zones, as shown in Figure 1. Specifically, WG1, WG2, and WG3 are positioned in deep water to measure incident waves, WG4 is placed in the reef-edge surf zone to record breaking waves, and WG5 and WG6 are located outside the surf zone to capture waves. Additionally, flow velocity in front of the toe of the structure is measured using a Vectrino-II 3D flowmeter combined with WG6 (see Fig. 2). Waves overtopping over the structure during the experiment were collected by a water inlet tray (20 cm wide tray placed at the centre of the structure crest) into the tank. The total volume of wave overtopping discharge is measured to determine the average overtopping discharge. Some images captured during the experimental process are presented in

Fig. 4. Images captured during the experimental process: (a) Test section in wave flume, (b) Wave gause and Vectrino-II 3-D flowmeter, (c) System collection waves overtopping, (d) Waves overtopping over dike crest

Fig. 4.

2.2. Experimental procedure

Experimental scenarios for a fringing reef model case are combined from different wave parameters and water depth on the reef flat. The variation range of these parameters must be wide enough, fully covering the actual conditions of the wave impact on the fringing reef so that the wave overtopping can occur from a small to large extent. The total number of test cases is 144, with the running test time for each test case being long enough to obtain at least 1000 single waves. Table 1 lists the scenarios that were combined for the tested models.

2.2.1. *Experimental wave scenarios*

Based on the statistical analysis of extreme waves in references [26, 27], the significant wave height (H_{m0}) ranges from 5.0 m to 8.0 m , while the peak wave period (T_p) varies between 8 s and 12 s . Considering a wide range of actual conditions in the study area and capacity of flume this experimental study considers wave parameters in Table 1. Random wave at boundary that produces a JONSWAP spectrum with $\gamma = 1.25$ and the common wave slope varies from 0.03 to 0.04 .

2.2.2. *Water depth on the reef flat*

The water depth (D) on the reef flat is defined as the vertical distance between the bottom of the reef flat and the water level. The scenarios for water depth on the reef flat were selected based on the actual characteristics of the fringing reef, with three scenarios for the water depths (d) set at 0.17 m, 0.20 m, and 0.23 m (see Table 1).

Table 1. Summary of experimental cases of wave overtopping

Water level		Physical models (slope tan α)	Wave parameter in deep water		Experiment time
d(m)	R_c(m)		H_{m0}(m)	T_p(s)	(minute)
0.17	0.18	MH1 : tan $\alpha = 1/2$	0.08	1.10	18
			0.08	1.30	22
			0.10	1.30	22
			0.10	1.50	25
			0.12	1.40	23
0.20	0.15	MH1-R: tan $\alpha = 1/2$+ roughness	0.12	1.60	27
			0.14	1.50	25
0.23	0.12	MH2: tan $\alpha = 1/3$	0.14	1.70	28
			0.16	1.60	27
		MH3: tan $\alpha = 1/4.27$	0.16	1.80	30
			0.18	1.70	28
			0.18	2.00	33
(Total: 3Rc × 4 Model × 12 Wave parameter = 144 cases)					

2.2.3. *Data processing*

Significant wave heights and spectral periods were defined following Eqs. (1) and (2):

$$H_{m0} = 4.004\sqrt{m_0} = 4.004\sqrt{\int_{f_L}^{f_U} S(f)df} \tag{1}$$

$$T_{m-1,0} = \frac{m_{-1}}{m_0} = \frac{\int_{f_L}^{f_U} f^{-1}S(f)df}{\int_{f_L}^{f_U} S(f)df} \tag{2}$$

Where f = wave frequency with lower frequency f_L = 0.025 Hz and upper frequency f_U = 2.5 Hz, S(f) = spectral density, m_{-1} and m_0 is the spectral moment.

The incident and reflected wave heights are calculated with the relation of the Eq. (3):

$$H_{m0,i} = \frac{H_{m0}}{\sqrt{1+K_R^2}} \tag{3}$$

The reflection coefficient in front of the toe of the structure is determined as the following Eq. (4) base on the research from Sheremet [10].

$$K_R^2 = \frac{F^-}{F^+}$$
$$F^{\pm} = \frac{1}{4}\sqrt{gd}\left[C_{oqn}(f) \pm (2\sqrt{d/g})C_{oqu}(f) + (d/g)C_{oul}(f)\right] \tag{4}$$

In which, F - and F+ are seaward and shoreward energy fluxes, respectively. $C_{o\eta}$ and C_{ouu} are wave and cross-shore velocity spectral density respectively; $C_{o\eta u}$ is η-u co-spectrum; d is water depth, g is gravity and f is frequency. The analysis of wave reflection utilized data recorded by a three-gauge array in the deep water, following the methodology outlined by J . Zelt and J. E. Skjelbreia [26].

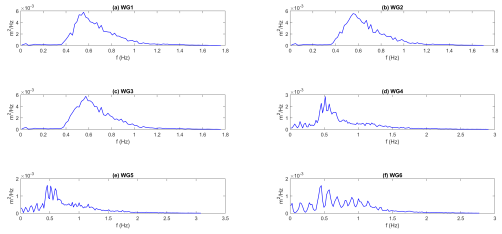

Fig. 5. Wave spectral transformation under H_{mo} = 0.16 m, T_p = 1.8 s(MH1)

Mean wave overtopping discharge q $\left(m^3/s/m\right)$ is calculated by the Eq.(5):

$$q = \frac{V_{ovt}}{t_0} \tag{5}$$

With V_{ovt} $\left(m^3\right)$ is total volume wave overtopping in during experimental period t_0(s).

3. Results and discussion

3.1. Characteristics of wave on the reef flat

When waves propagate across the fringing reef the effect of the reef-flat shallowness makes a transformation process and wave energy attenuation will occur due to the influence of effects such as wave breaking, and resonance triad interactions, bottom friction. In particular, the formation of IG waves is generated by the interaction of wave groups [27] and mainly due to fluctuations of the breaking point [28].

IG waves after forming in the breaking zone can also continue to develop due to triad interactions during propagation on the reef flat [3, 8]. Fig. 5 shows the strong transformation of the wave spectrum (MH1), showing the for-

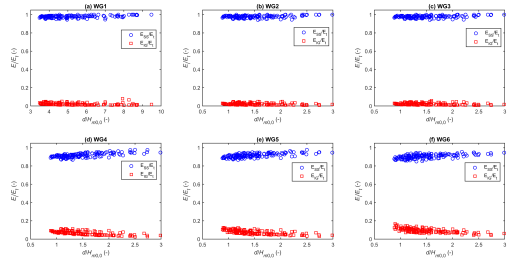

Fig. 6. The energy density of infragravity waves increases following the direction of wave propagation (from WG1 to WG6)

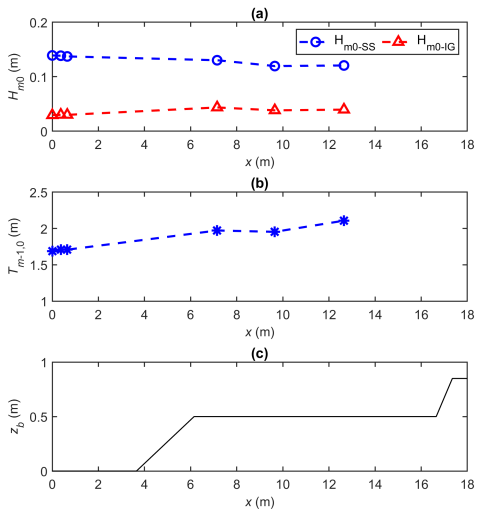

Fig. 7. Distribution of wave parameters under H_{m0} = 0.12 m, T_p = 1.6 s(MH1)

mation and development of IG waves on the fringing reef. Along the wave propagation direction, the energy of short wave (hereinafter denoted as SS) $\left(\left(E_{SS} \sim H_{m0} - SS^2\right)\right.$ is rapidly attenuated and therefore the energy of IG wave ($E_{IG} \sim H_{m0-IG}{}^2$) gradually has a significant proportion in the nearshore regions (accounting for 20% of the total wave energy in the nearshore regions, see Fig. 6). The role of IG waves needs to be appropriately included in the measurement of wave overtopping on the fringing reef.

The distribution of wave characteristics (H_{m0-SS}, H_{m0-IG}, and $T_{m-1,0}$) in case MH1-D20H12T16 in Fig. 7 shows the SS wave attenuating rapidly behind the breaking zone at the reef crest, while the IG wave tends to increase slightly. At an enough long distance close to the nearshore of fringing reef, the SS and IG wave heights remained stable. The characteristic spectral period increases slightly behind the breaking zone on the

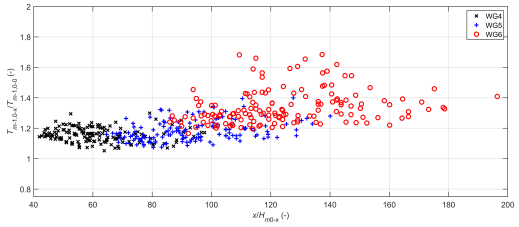

Fig. 8. Variation of the $T_{m-1,0}$ period along the reef flat

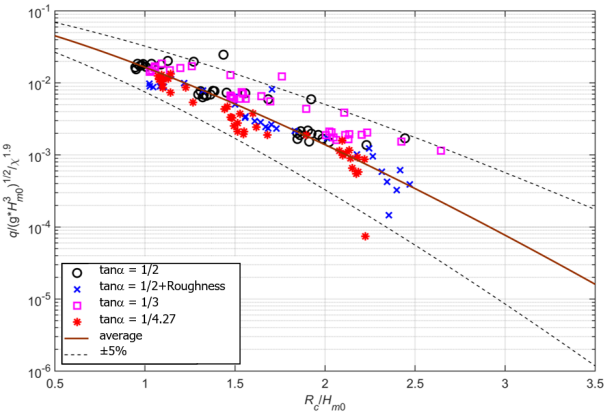

Fig. 9. Effect of slope on overtopping wave

nearshore of fringing reef (see Figure 8). The results show that the period $T_{m-1,0}$ is generally 1.1 - 1.7 times larger than that in the deep water and increases gradually in the direction of wave propagation. Waves in nearshore of fringing reefhave long periods due to the role of IG waves in this area. Effect of wave overtopping parameters over dikes on the fringing reef.

3.1.1. Relative crest freeboard, R_c/H_{m0}

The results presented above show the similarities to the wave overtopping over other traditional defended structures. Wave overtopping over sloping structures on the fringing reef is also inversely proportional to relative crest freeboard R_c/H_{m0} following the exponential rule (see Fig. 9). This is also the parameter that mainly influences the wave overtopping.

3.1.2. Wave steepness and wave period

Figure 10 shows the relationship between the dimensionless overtopping discharge $Q = q/\left(gH_{m0}\right)^3\Big)^{1/2}$ and the wave steepness $s_{m-1,0}$ with the same range of relative crest freeboard, R_c/H_{m0}. It can be seen that, unlike EurOtop-2018 for non-breaking waves, the wave period has a certain influence on the overtopping wave over the structure. With the same R_C/H_m, the longer the wave, the larger the

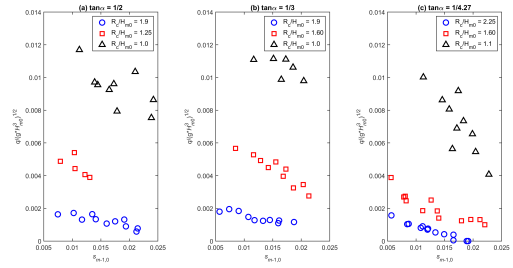

Fig. 10. Effect of wave steepness and wave period on overtopping wave

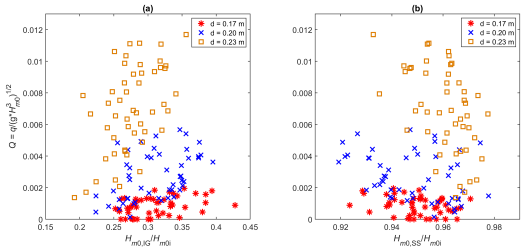

Fig. 11. Correlation between wave overtopping discharge and density of IG wave and SS wave; (a) $Q \sim H_{m0,IG}/H_{m0}$; (b) $Q \sim H_{m0,SS}/H_{m0i}$

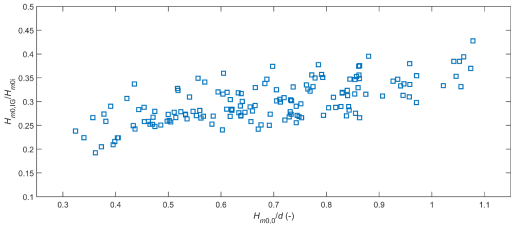

Fig. 12. The increase in the proportion of IG waves (at WG6) is influenced by the relative reef-flat shallowness $H_{m0,0}/d$

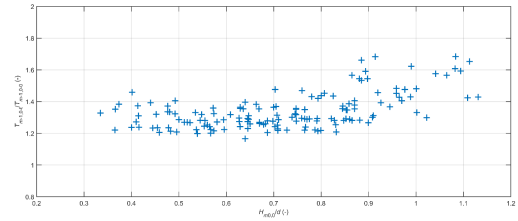

Fig. 13. Effect of $H_{m0,}/d$ on the characteristic spectral period in front of the toe of the structure.

overtopping wave will be. The effect of the wave period becomes larger when R_c/H_{m0} is smaller (relative slope $Q \sim s_{m-1,0}$ is larger). In addition, the results in Figure 10 show a clear influence of structure slope, especially when R_c/H_{m0} is large $(R_c/H_{m0} > 1.0)$.

3.1.3. Effects of the relative reef-flat shallowness and infragravity waves

The relative reef-flat shallowness (i.e., the ratio of the water depth over the reef flat (d) to the offshore incident wave height $(H_{m0,0})$, $H_{m0,0}/d$ is a parameter that has an important influence on the wave hydrodynamic properties on the fringing reef [25, 29]. The relative reef-flat shallowness has a dominant influence on the formation and development of IG waves, wave setup, and the relative proportion of SS wave and IG wave compared to the total wave energy, as shown in Fig. 6 [3, 7].

Fig. 11 shows the correlation from experimental data between the dimensionless overtopping discharge Q and the IG and SS wave height densities in the total wave height (incident wave determined in front of the structure at wave gauges WG6). It can be seen that although the long wave has a rather small density in the total wave $(H_{m0,IG}/H_{m0i} = 0.2 - 0.4$, Fig. 11a), the wave overtopping discharge is quite sensitive to the increase in the density of the IG wave, Q increases rapidly when $H_{m0,IG}/H_{m0i}$ increases with each case of water depth on the reef flat (crest freeboard R_c). Whereas short waves account for a large proportion of the total wave and have less variation $(H_{m0,SS}/H_{m0i} = 0.92 - 0.98$, Fig. 11b). However, in the opposite direction, the wave overtopping discharge tends to decrease when the proportion of SS wave in the total wave increases.

The proportion of IG wave height in the total wave H_{m0-IG}/H_{m0i} (at WG6) is ultimately dominated by the relative reef-flat shallowness $H_{m0,0}/d$ as shown in Fig. 12. In general, the density of IG wave increases when the shallowness of the reef flat increases, that is, the difference between the wave height in deep water and the water depth on the reef flat is larger. This is also consistent with previous studies as described above. Besides that, the influence of the ratio $H_{m0,0}/d$ on the overtopping is through the distortion of the wave spectrum (frequency redistribution) which is reflected through the characteristic period of the spectrum, $T_{m-1,0}$, at the front of the structure (WG6), as shown in Fig. 13. Accordingly, the ratio $T_{m-1,0-t}/T_{m-1,0-0}$ increases when the relative reef-flat shallowness $H_{m0,0}/d$ increases. Basically, the effect of wave period or wave steepness (see Fig. 10) on the wave overtopping is reflected through the shallowness of the reef flat.

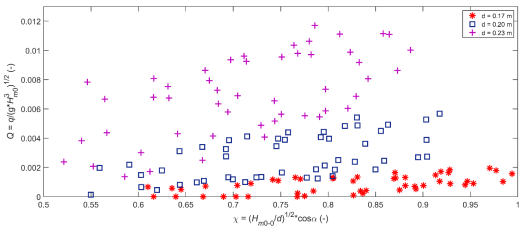

Fig. 14. The dependence of the dimensionless overtopping discharge (Q) on the synthetic effect parameter (χ)

3.1.4. *The synthetic effect parameter* (χ)

As analyzed above, the wave overtopping over dikes on the fringing reef depends on the relative crest freeboard R_c/H_{m0}, the relative reef-flat shallowness $H_{m0,0}/d$, and the slope of the dikes. In this study, we propose a new parameter χ :

$$\chi = \left(\frac{H_{m0,0}}{d}\right)^{1/2} \cos\alpha \tag{6}$$

From Eq. (6), the dependence of the dimensionless overtopping discharge Q on χ from the experimental data is shown in Figure 14 for each case of different water levels. It is clear that Q tends to increase slightly when χ increases.

3.2. Development of a new empirical formula for wave overtopping over a sloping structure on a fringing reef

Waves overtopping over sloping structures (dikes, breakwaters) are divided into two cases: Breaking and non-breaking waves on the slope of structures. Wave overtopping discharge mainly depends on the relative crest freeboard R_c/H_{m0}. In case of wave breaking, the overtopping discharge depends on the Iribarren number. The average overtopping discharge is determined for each case as follows Eqs. (7) and (8):

Breaking wave $(\xi_{m-1,0} \leq 2.0)$:

$$\frac{q}{\sqrt{gH_{m0}^3}} = \frac{0.023}{\sqrt{\tan\alpha}}\xi_{m-1,0}\exp\left[-\left(2.7\frac{R_c}{\xi_{m-1,0}H_{m0}}\right)^{1.3}\right] \tag{7}$$

Non-breaking wave $(\xi_{m-1,0} > 2.0)$:

$$\frac{q}{\sqrt{gH_{m0}^3}} = 0.09\exp\left[-\left(1.5\frac{R_c}{H_{m0}}\right)^{1.3}\right] \tag{8}$$

In which, q is the mean overtopping discharge per meter structure width $(\mathrm{m^3/s/m})$; R_c is the crest freeboard of structures; α is the slope of the front face of the structure; H_{m0} is incident wave height at the toe of structures; $\xi_{m-1,0}$ is Iribarren number is defined by Eq. (9):

$$\xi_{m-1,0} = \frac{\tan\alpha}{\sqrt{\frac{2\pi H_{m0}}{gT_{m-1,0}^2}}} \tag{9}$$

Note that in the above formulas, in the case study, influence for the roughness of or on the slope, oblique wave attack, a berm, and vertical wall on the slope are ignored. The reliability of Eq. (7) is given by $\sigma(0.023) = 0.003$ and $\sigma(2.7) = 0.20$, and of Eq. (8) by $\sigma(0.09) = 0.0135$ and $\sigma(1.5) = 0.15$. From these values, a 90% or 95% confidence band can be constructed.

It can be seen that the majority of experimental data $(123/150)$ are seen in the case of non-breaking waves. This is because the wave period becomes longer with the appearance of IG waves on the slope of the structure. The data points fall into the case of wave breaking on the slope when the wave has a short period (where the relative water depth on the slope is large, the wave breaks less on the slope and has little variation) and the structure has a gentle slope $(\tan\alpha = 1/4.27)$. Therefore, in this study, we will consider all the data together without distinguishing between breaking and non-breaking waves on the slope of the structure.

From the correlation analysis about the dominance of the parameters in the above sections and based on the formula for calculating the wave overtopping over the dikes on the beach of EurOtop-2018 Eq. (8) , the empirical formula for calculating the wave overtopping over the dikes on the fringing reef is proposed as follows Eq. (10):

$$Q = \frac{q}{\sqrt{gH_{m0}^3}} = a\cdot\chi^m\cdot\exp\left[-\left(b\cdot\frac{R_c}{H_{m0}}\right)^c\right] \tag{10}$$

In which, band c are the experimental coefficients as determined by Eq. (8), a and m are the experimental coefficients determined according to the results of regression analysis with experimental data for the case fringing reef. To adjust Eq. (8) with additional consideration of fringing reef influencing factors, the coefficients b and c will need to be kept the same (i.e. $b = 1.5$ and $c = 1.3$), a and m will be determined based on the experimental data set of the study.

Transform from Eq. (10), it is rewritten as below:

$$Q_R = \frac{q}{\sqrt{gH_{m0}^3}}\cdot\exp\left[\left(b\cdot\frac{R_c}{H_{m0}}\right)^c\right] = a\cdot\chi^m \tag{11}$$

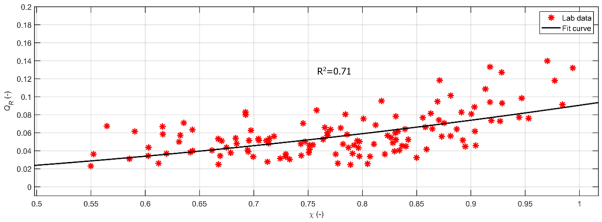

Fig. 15. Regression analysis relationship between Q ~ χ

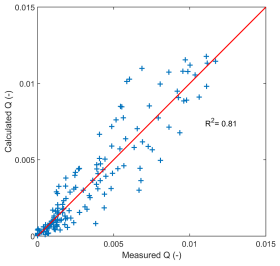

Fig. 16. Comparison between experimental and calculated data.

The results of the regression analysis of Eq. (11) with experimental data are shown in Fig. 15. The empirical coefficients in Eq. (10) are determined as $m = 1.90$ and $a = 0.090\ (0.085, 0.096)$. Interestingly, the empirical coefficient a is constant compared to the original Eq. (8) of EurOtop-2018 $(a = 0.09)$. Finally, Eq. (10) is rewritten as:

$$Q = \frac{q}{\sqrt{gH_{m0}^3}} = 0.09 \cdot \exp\left[-\left(1.50\frac{R_c}{H_{m0}}\right)^{1.30}\right] \cdot \chi^{1.90} \tag{12}$$

Thus, compared with Eqs. (8) and (12) differs only in the last term on the right $(\chi^{1.90})$ which accounts for the difference in wave hydrodynamics on fringing reefs compared to the case on beaches. Figure 16 shows the results of calculating the dimensionless overtopping discharge Q according to Eq. (12) when compared with the experimental data. The agreement between experimental calculations is quite good $(R^2 = 0.81)$.

Wave overtopping data according to Eq. (12) and shown in Fig. 17 . It can be seen that, with the new experimental formula, the experimental data points have significantly reduced dispersion and are quite well concentrated around the mean regression line. The wave overtopping Eq. (12) has the scope of an application according to the variation range of the experimental parameters as follows:

Crest relative freeboard: $R_c/H_{m0} = 0.95 - 3.15$

Relative reef-flat shallowness: $H_{m0,0}/d = 0.32 - 1.08$

Incident wave height in deep water boundary: $H_{m0,0} = 3.0 - 8.5$ m

Incident wave period in deep water boundary: $T_{m-1,0} = 6.5 - 13.5$ s

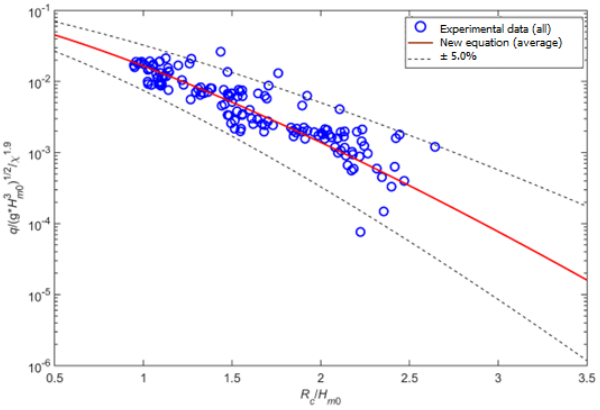

Fig. 17. Data of wave overtopping over dikes on the fringing reef.

4. Conclusion

The paper investigates and enhances the calculation methodology for wave overtopping over a dike on fringing reefs during both design and flood assessment in areas built on fringing reefs through physical model experiments. These experiments were elaborately conducted in the wave flume with 144 scenarios, combining four physical models with various wave and still water levels.

The research results demonstrate a significant transformation of waves as they propagate from deep water areas to shallow water reef flats, particularly the formation of IG waves with wave periods increasing from 1.1 to 1.7 times the deep-water wave period. The contribution of IG wave energy increases to approximately 20% of the total wave energy in the toe of the area, and this contribution is proportional to the wave overtopping discharge.The wave overtopping over the dikes on the fringing reef, in addition to the dominant influence of the relative crest freeboard, also depends on a synthetic parameter which typical for the wave hydrodynamic properties that affect the wave overtopping on the fringing reef.

An empirical formula Eq. (12) for wave overtopping over dikes on the fringing reef based on the original formula of EurOtop-2018 for dikes on beaches in case of non-breaking waves. This is a new formulation and a dedication of the paper on theoretical development.

Eq. (12) has been practically applied to calculate the wave overtopping over dike on the fringing reef and to mitigate wave-overtopping,ensuringthe safety of the struc-

tures on fringing reefs in Vietnam. Currently, the systems to mitigate wave-overtopping is working well. This formula can be applied to other fringing reefs in different areas with wave parameters in deep water boundaries: $H_{m0,0} = 3.0 - 8.5$ m, $T_{m-1,0} = 6.5 - 13.5$ s, relative reef-flat shallowness: $H_{m0,0}/d = 0.32 - 1.08$ and crest relative freeboard: $R_c/H_{m0} = 0.95 - 3.15$.The study of wave overtopping over a dike on a fringing reef has positive results. However, the study has so far only considered the one-dimensional problem and simple structure forms. The research direction will continue to investigate the influence of three-dimensional problems and complex structure forms, and providing solutions to mitigate wave overtopping over structures.

References

[1] E. Beetham and P. S. Kench, (2018) *"Predicting wave overtopping thresholds on coral reef-island shorelines with future sea-level rise"* **Nature Communications *9***(1): 3997. DOI: 10.1038/s41467-018-06550-1.

[2] Y. Liu, Z. Liao, K. Fang, and S. Li, (2021) *"Uncertainty of wave runup prediction on coral reef-fringed coasts using SWASH model"* **Ocean Engineering *242***: 110094.

[3] A. Pomeroy, R. Lowe, G. Symonds, A. Van Dongeren, and C. Moore, (2012) *"The dynamics of infragravity wave transformation over a fringing reef"* **Journal of Geophysical Research: Oceans *117***(C11):

[4] Q. C. Dinh, Q. T. Nguyen, D. D. Ho, and C. T. Mai, (2023) *"Effects of bottom roughness on wave transmission across a submerged reef"* **Frontiers in Marine Science *10***: 1113195.

[5] K. Splinter, L. Li, and M. Blacka, (2018) *"Laboratory Experiments Of Wave Overtopping Of Revetment Structures In Reef Environments"* **Coastal Engineering Proceedings** (36): 80–80.

[6] S. K. Paul and W. B. Robert, (2006) *"Wave Processes on Coral Reef Flats: Implications for Reef Geomorphology Using Australian Case Studies"* **Journal of Coastal Research 22**(1): 209–223.

[7] M. L. Buckley, R. J. Lowe, J. E. Hansen, and A. R. Van Dongeren, (2015) *"Dynamics of Wave Setup over a Steeply Sloping Fringing Reef"* **Journal of Physical Oceanography *45***(12): 3005–3023. DOI: 10.1175/jpo-d-15-0067.1.

[8] O. Nwogu and Z. Demirbilek, (2010) *"Infragravity wave motions and runup over shallow fringing reefs"* **Journal of Waterway, Port, Coastal, and Ocean Engineering *136***(6): 295–305.

[9] J. M. Becker, M. A. Merrifield, and M. Ford, (2014) *"Water level effects on breaking wave setup for Pacific Island fringing reefs"* **Journal of Geophysical Research: Oceans *119***(2): 914–932. DOI: https://doi.org/10.1002/2013JC009373.

[10] A. Sheremet, R. Guza, S. Elgar, and T. Herbers, (2002) *"Observations of nearshore infragravity waves: Seaward and shoreward propagating components"* **Journal of Geophysical Research: Oceans *107***(C8): 10-1-10–10.

[11] V. Roeber and J. D. Bricker, (2015) *"Destructive tsunami-like wave generated by surf beat over a coral reef during Typhoon Haiyan"* **Nature Communications *6***(1): 7854. DOI: 10.1038/ncomms8854.

[12] O. M. Cheriton, C. D. Storlazzi, and K. J. Rosenberger, (2016) *"Observations of wave transformation over a fringing coral reef and the importance of low-frequency waves and offshore water levels to runup, overwash, and coastal flooding"* **Journal of Geophysical Research: Oceans *121***(5): 3121–3140. DOI: https://doi.org/10.1002/2015JC011231.

[13] C. D. Storlazzi, W. J. Skirving, J. J. Marra, R. T. McCall, and A. W. Pomeroy, (2021) *"Flooding on coral reef-lined coasts: Current state of knowledge and future challenges"* **Frontiers in Marine Science**:

[14] M. A. Merrifield, J. M. Becker, M. Ford, and Y. Yao, (2014) *"Observations and estimates of wave-driven water level extremes at the Marshall Islands"* **Geophysical Research Letters *41***(20): 7245–7253. DOI: https://doi.org/10.1002/2014GL061005.

[15] H. Burchartch and S. Hughes. *Coastal Engineering Manual, Fundamentals of design.* Vicksburg, USA: US Army Corps of Engineering, 2003.

[16] J. De Rouck, C. Boone, and B. Van de Walle. *The optimisation of crest level design of sloping coastal structures through prototype monitoring and modelling, final report*. Report. 2001.

[17] J. W. van der Meer, H. Verhaeghe, and G. J. Steendam, (2009) *"The new wave overtopping database for coastal structures"* **Coastal Engineering *56***(2): 108–120. DOI: https://doi.org/10.1016/j.coastaleng.2008.03.012.

[18] J. W. Van der Meer, (1995) *"Wave run-up and wave overtopping at dikes"* **ASCE**:

[19] J. Van der Meer, N. Allsop, T. Bruce, J. De Rouck, A. Kortenhaus, T. Pullen, H. Schuttrumpf, P. Troch, B. Zanuttigh, et al., (2016) *"EurOtop-Manual on wave overtopping of sea defences and related structures. An overtopping manual largely based on European research, but for worldwide application."*

[20] C. Altomare, T. Suzuki, X. Chen, T. Verwaest, and A. Kortenhaus, (2016) *"Wave overtopping of sea dikes with very shallow foreshores"* **Coastal Engineering *116***: 236–257. DOI: https://doi.org/10.1016/j.coastaleng.2016.07.002.

[21] Y. Liu, S. Li, S. Chen, C. Hu, Z. Fan, and R. Jin, (2020) *"Random wave overtopping of vertical seawalls on coral reefs"* **Applied Ocean Research *100***: 102166.

[22] Y. Liu, S. Li, X. Zhao, C. Hu, Z. Fan, and S. Chen, (2020) *"Artificial neural network prediction of overtopping rate for impermeable vertical seawalls on coral reefs"* **Journal of Waterway, Port, Coastal, and Ocean Engineering *146***(4): 04020015.

[23] Y. Gao, L. Ren, and L. Wang, (2023) *"Experimental Investigation of Wave Propagation and Overtopping over Seawalls on a Reef Flat"* **Journal of Marine Science Engineering *11***(4): 836.

[24] T. Q. Tuan and D. Q. Cuong. "Wave transmission across steep submerged reefs". In: *APAC 2019: Proceedings of the 10th International Conference on Asian and Pacific Coasts, 2019, Hanoi, Vietnam*. Springer, 687–694.

[25] T. Q. Tuan and D. Q. Cuong, (2019) *"Distribution of wave heights on steep submerged reefs"* **Ocean Engineering *189***: DOI: 10.1016/j.oceaneng.2019.106409.

[26] J. Zelt and J. E. Skjelbreia, (1992) *"Estimating incident and reflected wave fields using an arbitrary number of wave gauges"* **Coastal Engineering 1992**: 777–789.

[27] J. A. Battjes, H. J. Bakkenes, T. T. Janssen, and A. R. van Dongeren, (2004) *"Shoaling of subharmonic gravity waves"* **Journal of Geophysical Research *109***(C2): DOI: https://doi.org/10.1029/2003JC001863.

[28] T. E. Baldock, (2012) *"Dissipation of incident forced long waves in the surf zone—Implications for the concept of "bound" wave release at short wave breaking"* **Coastal Engineering *60***: 276–285. DOI: https://doi.org/10.1016/j.coastaleng.2011.11.002.

[29] B. Hofland, X. Chen, C. Altomare, and P. Oosterlo, (2017) *"Prediction formula for the spectral wave period Tm-1,0 on mildly sloping shallow foreshores"* **Coastal Engineering *123***: 21–28. DOI: https://doi.org/10.1016/j.coastaleng.2017.02.005.